SCALE AND HETEROGENEITY IN HYDRAULIC PROPERTIES OF THE FRACTURED GRANITIC BOISE FRONT, BOISE, IDAHO

by

Bernadette Acker Hoffman

A thesis

submitted in partial fulfillment

of the requirements for the degree of

Master of Science in Geology

Boise State University

April 2008

The thesis presented by Bernadette Acker Hoffman entitled Scale and heterogeneity in hydraulic properties of the Dry Creek Experimental Watershed, Boise, Idaho is hereby approved:

James McNamara Advisor	Date
Clyde Northrup Committee Member	Date
David Wilkins Committee Member	Date
John R. (Jack) Pelton Dean of the Graduate College	Date

ACKNOWLEGEMENTS

My completion of this thesis is only the result of support in many different forms by many individuals. I would like to thank my committee members; Dr. James McNamara, Dr. David Wilkins, and Dr. C.J. Northrup; for their innovative ideas, insight and advice on this project. I would also like to thank them for allowing me so much independence throughout my graduate career.

Contributions and advice by Dr. Warren Barrash and Dr. Tom Clemo allowed me to continue forward in many instances where I wasn’t sure I could. Thank you both for the time you took to answer my questions.

Pam Aishlin proved a truly patient and uncomplaining field assistant in hot, dry, dusty, and steep conditions. Her sense of humor often kept me going.

This project was funded by the NSF-Idaho EPSCoR Program and the National Science Foundation (Award Number: EPS-0447689), the NASA EPSCoR Idaho Space Grant Fellowship, and the Boise State University Department of Geosciences which provided a research assistantship.

Karen Viscupic and many others of the Department of Geosciences provided answers to questions regarding every topic I had a question for and I thank them.

I would like to sincerely thank my family for encouraging me and supporting me in every endeavor throughout my life. Their love and support is largely responsible for getting me to this station in my life and I’m very grateful to have them.

Finally, I am grateful to my loving husband who never complained when I worked long hours and weekends, who’s belief in me never wavered, who’s support in every way allowed me to grow both academically and creatively.

ABSTRACT

A continuum approach model was used to determine the permeability of the fractured granite Idaho Batholith underlying the Dry Creek Experimental Watershed east of Boise, Idaho and characterization of the fracture network was completed. A technique for applying the apertures of fractures measured in a less weathered area to the fracture network in the (DCEW) is described. A Monte Carlo simulation of permeability showed that a Representative Elemental Volume (REV) does exist in the DCEW. Plotting the permeability calculated stochastically in the Monte Carlo simulation against the summed outcrop area shows a distinct plateau around 10^{-6} m^2 which is larger than the estimate of the permeability, 10^{-9} m^2, using the traditional REV plot but very similar to the deterministic calculation of the permeability of 1.49×10^{-6} m^2 using the continuum model. The Monte Carlo simulation has the advantage over the traditional REV plot in that outcrops with large area are well represented and the estimate of the plateau is based on more than just a few measurements.

TABLE OF CONTENTS

INTRODUCTION

Many intermountain west cities with arid to semi-arid climates, such as Boise, Idaho, rely on mountain block recharge (MBR) to deliver water from mountain snow pack to adjacent valley aquifers. MBR is divided into two components: (1) subsurface inflow from the mountain block and (2) infiltration from perennial and ephemeral streams near the mountain front. Of these components estimates of subsurface inflow are the most poorly constrained (Manning and Solomon, 2003). Hutchings and Petrich (2002) found that recharge to deep aquifer flow systems under Boise likely occurs as underflow from the Atlanta Lobe of the Idaho Batholith, a composite mass of fractured granitic plutons occurring north and east of the city that were emplaced from the Jurassic to the Eocene (Criss and Champion, 1984).

The difficulty in constraining subsurface inflow and the mechanisms of MBR have been the subject of numerous investigations in the Boise Front northeast of Boise in the Dry Creek Experimental Watershed (DCEW) (Figure 1) a highly studied watershed of 28 km^2 area, which was used as the laboratory for this investigation (Aishlin, 2006; Morgos, 2006, Williams, 2005). Previous investigations in the DCEW have revealed the hydraulic properties of the bedrock to be highly heterogeneous and Aishlin (2006) found that up to 11% of the annual rainfall is partitioned to groundwater recharge. The heterogeneity of hydraulic properties is key to understanding deep subsurface flow and,

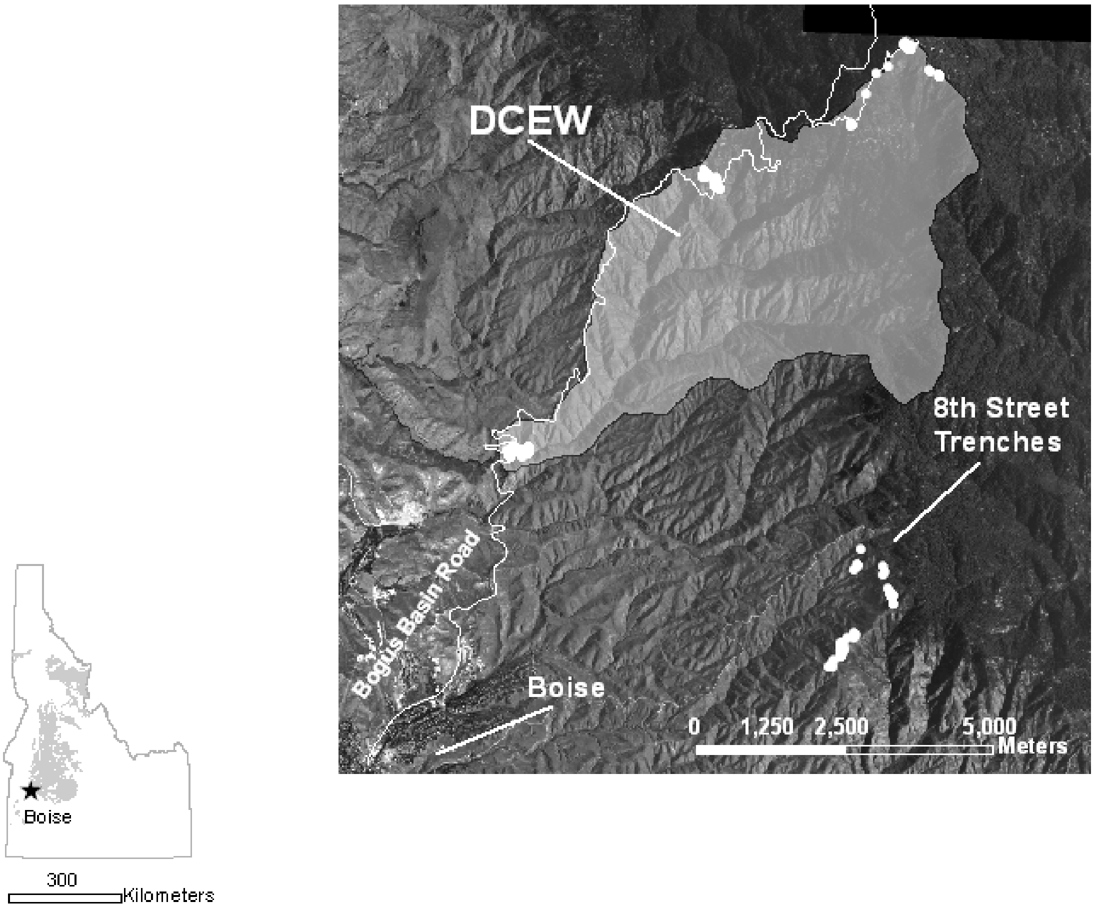

Figure 1: Study area location map. The grey region in the inset map shows the extent of the Idaho Batholith and the black star marks Boise, Idaho. The Dry Creek Experimental watershed is shown in the larger map outlined by the grey region. White dots indicate sampling locations in the DCEW and the 8th Street Trenches. The DCEW begins at the junction of Dry Creek Watershed and Bogus Basin Road and extends to the upper 11 km of Dry Creek.

therefore, the full description of MBR in this watershed. This problem is compounded by the fact that bedrock is fractured granite. Hydraulic properties of fractured crystalline rocks vary within a single fracture, between adjacent fractures, between nearby outcrops and over the scale of a watershed.

The bedrock outcrops occurring in the Dry Creek Experimental Watershed (DCEW) are highly weathered and rounded, especially in fractures producing gaping apertures. This weathering is typical of the Atlanta Lobe of the Idaho Batholith which was subjected to rapid downcutting in the last 10 Ma as inferred by fission track dating (Sweetkind and Blackwell, 1989). This has left a landscape epitomized by deeply incised canyons and steep slopes (Clayton et al., 1979).

The high degree of weathering complicates strategies to investigate the hydraulic properties of the bedrock in the DCEW. Steep slopes have prohibited many types of hydraulic and geophysical investigation techniques; however, field mapping was a cost-effective and attractive approach.

To model permeability, complete characterization (including length, aperture, orientation, and location of individual fractures in a network) is necessary (Long and Witherspoon, 1985). Often the choice of a model depends on what data is available from field reconnaissance. In the case of the DCEW, the highly weathered outcrops afforded very little data. Therefore, complete characterization required extracting data from other sources and applying it to the DCEW.

The objective of this investigation is to calculate a bulk permeability of the fractured rock mass of the DCEW. Permeability is a measure of the ease with which a porous medium transmits water (Fetter, 2001). It is most often measured in the laboratory using drilling cores. However there are two problems with doing this in the DCEW. First, these measurements are point measurements that do not easily lend themselves to upscaling to the entire watershed. Second, drilling would be nearly impossible in the steep terrain of the DCEW which is typical of the rest of the Atlanta Lobe of the Idaho Batholith with 1,100 m difference between the headwaters and Dry Creek's junction with Bogus Basin Road, the boundary of the experimental watershed (Williams, 2005). Because drilling is logistically difficult and out of budget for this investigation, pump tests could also not be used to measure the permeability of the DCEW. The most cost-effective solution for this investigation is to map the fractures in the field and then model the results.

Modeling of fractures from field reconnaissance lends itself far better to upscaling than other methods, and it does not have the logistical or cost drawbacks associated with drilling. However, outcrops in the DCEW are sparse and concentrated primarily on south-facing slopes of the watershed. To check that this outcrop pattern does not create a bias in the fracture sets measured in the field, remote sensing is used to extend the field mapping over the entire area of the watershed.

The field data are first checked against the lineaments extracted from aerial photographs to ascertain the appropriateness of upscaling and then the permeability of individual outcrops is estimated using the continuum approach model to calculate the permeability of the entire watershed stochastically as well as deterministically. Using a continuum approach model deterministically can not describe scale breaks or patterns with increasing scale, therefore upscaling of the field data is also investigated stochastically using a Monte Carlo simulation to incrementally upscale permeability.

BACKGROUND

The DCEW is located 16 km northeast of Boise, Idaho within the Boise Front. Dry Creek is a perennial stream flowing south to southeast through steep mountainous terrain in a semiarid climate. The headwaters are at an elevation 2100 m and the DCEW includes the watershed surrounding the upper 11 km of Dry Creek to its junction with Bogus Basin Road. Dry Creek is instrumented at multiple sites for ongoing investigations in hydrology, geochemistry, mathematics, and engineering. The terrain of the DCEW typifies that of the Atlanta Lobe of the Idaho Batholith in that it is steep and strongly dissected by streams (Williams, 2005).

The highly weathered, rounded outcrops in the DCEW complicated characterization of the fracture network especially length and aperture measurements. Because measurement of aperture was impossible in the DCEW due to weathering, fresh bedrock exposure close to the DCEW needed to be found. An area known as the 8th Street trenches was attractive because it offered fresh outcrop exposures as the bedrock had been exposed in the last 10 years. Trenches were dug perpendicular to slopes to prevent mass wasting after a range fire east of Boise and just south of the DCEW. In some locations along these trenches excavators dug through the rock exposing fresh surfaces. The apertures and orientations of these fractures could be measured and applied to the fractures in the DCEW to aid in modeling fracture permeability.

Two approaches to model fracture permeability from field mapping data exist: the continuum approach which is also called the porous media equivalent approach and the discrete fracture network (DFN) approach. The continuum approach assumes fractures to be infinite in length and an equivalent porous media tensor is calculated (Long and Witherspoon, 1985). The DFN approach, on the other hand, uses the statistical properties of the size and orientation of the network to calculate the transmissivity of the individual fractures as well as calculate the connectivity of the network based on the size distribution and density (Long and Witherspoon, 1985; Dershowitz et al., 2004). A comparison of these two modeling approaches used on the same fracture population would be invaluable; however, it is beyond the scope of this investigation and will be the topic of future work. This investigation will focus on the fracture network characterization and flow modeling with a continuum approach model. These will contribute to the description of MBR in future work in the DCEW.

Continuum approach

The continuum or porous media equivalent approach was initially proposed by Snow (1965) who developed a mathematical expression for flow through a single fracture in the laboratory with the use of parallel glass plates. The derivation is based on the Navier-Stokes equations for single-phase, non-turbulent flow and assumes that the flow is governed by Darcy’s Law (Gale, 1982). This model assumes fractures are infinite in length and an equivalent porous medium tensor is calculated by accumulating the permeabilities of the individual fractures to estimate an average permeability (Long et al., 1982).

The Navier-Stokes equation is the 3D balance equation for linear momentum of an incompressible fluid and takes the form

$$\rho \frac{\partial \mathbf{V}}{\partial t} + \rho \nabla \cdot \left(\mathbf{V} \bullet \nabla \mathbf{V} \right) + \nabla p - \rho \mathbf{g} - \mu \nabla^2 \mathbf{V} = 0 \qquad (1)$$

where ρ is density, μ is viscosity, V it the fluid's mass weight velocity, t is time, p is pressure, and g is gravitational acceleration ($g = -g\nabla z$, where z is the vertical coordinate) (Bear et al., 1993). Because the velocity vector points in the x-direction and varies only in the z-direction a simplification arises so that the velocity vector of flow between two smooth parallel plates is given as (Zimmerman and Yeo, 2000):

$$u_x = -\frac{1}{2\mu} \frac{dP}{dx} \left[z^2 - \left(\frac{h}{2} \right)^2 \right], u_z = 0 \qquad (2)$$

Integrating the velocity profile across the fracture gives the overall flowrate (Zimmerman and Yeo, 2000)

$$Q_x = \int_0^w \int_{-h/2}^{h/2} u_x(z) dz dy = -w \int_{-h/2}^{h/2} \frac{1}{2\mu} \frac{dP}{dx} \left[z^2 - \left(\frac{h}{2} \right)^2 \right] dz = \frac{-wh^3}{12\mu} \frac{dP}{dx} \qquad (3)$$

where w is the depth of the fracture in the direction perpendicular to the flow direction.

This leads to the cubic law as Q_x=-(T/μ)(dP/dx), therefore

$$T = \frac{wh^3}{12} \tag{4}$$

where T is the transmissivity (Zimmerman and Yeo, 2000).

To scale up the transmissivity for a group of randomly oriented fractures, let ς be the average hydraulic conductivity gradient and ς^* is the average driving force in the fracture plane such that $\varsigma^* = \varsigma - (\varsigma \cdot \nu)\nu$.

$$\varsigma_j^* = \sum_{i=1}^{3} \varsigma_i \left(\delta_{ij} - \nu_i \nu_j\right), \quad i, j = 1,2,3, \tag{5}$$

where v_{ij} is the matrix of the direction cosines of the normal to each fracture and   is the Kronecker delta. The average velocity at a point in a fracture is $\tilde{V}$ and

$$\tilde{V} = K_{fr} \varsigma_j^* = K_{fr} \left(\delta_{ij} - \nu_i \nu_j\right) \varsigma_i, \quad i, j = 1,2,3, \tag{6}$$

where K_{fr} is the hydraulic conductivity in an individual fracture. The hydraulic conductivity of a fracture domain is obtained by averaging equation 6 over the void space in the representative elemental volume (REV) by integrating (6) and dividing by the volume of the REV denoted by U_o in equation 7 below

$$\overline{V}_j \equiv \frac{1}{U_o} \int_{(U_{ov})} V_j dU = \frac{1}{\Sigma A} \int_{(\Sigma A)} \tilde{V}_j dA = \frac{1}{\Sigma A} \int_{(\Sigma A)} K_{fr} \left(\delta_{ij} - \nu_i \nu_j\right) \varsigma_i dA \tag{7}$$

where U_{ov} is the volume of the void space in U_o, A is the fracture surface area in U. Using the symbol <…> to denote average over the total surface are of the fractures then (7) can be written

$$\bar{V}_j = < K_{fr}\left(\delta_{ij} - \nu_i \nu j\right) > \varsigma_i \tag{8}$$

and the overall specific discharge q_{ij} is (Bear et al., 1993)

$$q_j \equiv \phi \bar{V}_j = \phi_{fr} \overline{K_{fr}\left(\delta_{ij} - \nu_i \nu_j\right)} \varsigma_i \equiv \left(K^*_{fr}\right)_{ij} \varsigma_i \tag{9}$$

where $(K^*_{fr})_{ij} = \phi_{fr} < K_{fr}\left(\delta_{ij} - \nu_i \nu_j\right) > and\, \phi_{fr} = < b > \Sigma A / U_o$.

In order to estimate an average permeability, a volume must exist where the permeability ceases to vary with an increase in volume; the definition of the concept of Representative Elemental Volume (REV) first discussed by Hubbert (1956) (Long et al.,1982). Figure 2 is the traditional graphical representation of the REV concept such that permeability varies greatly at small scales and then plateaus when the REV is achieved. Further increases in volume do not result in change to the permeability. One weakness in creating a plot like Figure 2 is that often there are far fewer outcrops forming the right hand side of the figure, larger than the REV, than smaller than the REV. This begs the question whether the REV is a result of a real decrease in heterogeneity or if it appears that way because there are so few outcrops with large volumes in the sample.

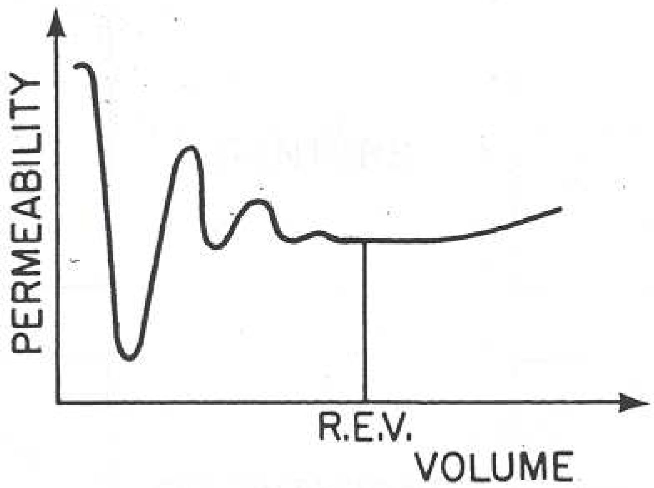

Figure 2: Variation of permeability with increasing domain volume (Hubbert, 1956).

An REV often does not exist for fractured media because heterogeneity occurs over a broad range of scales (Hsieh, 1998). The lack of an REV suggests limitations in using a continuum approach model for calculating transmissivity and permeability (Berkowitz, 2002).

The transmissivity and, in turn, the permeability of a fracture network is a function of the tranmissivity of the individual fractures comprising the network and how connected the individual fractures are, termed the connectivity (Long and Witherspoon, 1985). Connectivity is a function of a fracture network’s size distribution and the spatial density of the fractures (Renshaw, 1999). Based on these concepts it’s clear that the continuum approach will overestimate the permeability of a fracture network because it does not account for network connectivity (Long et al., 1982).

DFN approach

The recognition of the importance of fracture network connectivity in modeling permeability led to the development of DFN models that could account for this (Long et al., 1982; Long and Witherspoon, 1985; Oda, 1984). Connectivity is described by the spatial density and the length distribution of the fractures (Renshaw, 1999). There are many DFN models currently in use and each one uses a joint system model to locate fractures and then the probability density function of the fracture lengths to limit the flow to the actual area of the fracture (Long and Witherspoon, 1985; Dershowitz et al., 2004). Mesh generators or finite element solutions are used to discretize flow in each fracture and the Laplace equation is solved for each discrete fracture. Intersections are treated as either sources or sinks and global mass balance equations ensure conservation of mass (Long et al., 1982; Dershowitz et al., 2004).

DFN models begin with a fracture network model or joint system model which places fracture centers within a domain of a predetermined size that is 1D, 2D or 3D and dictates the shape of the modeled fractures. Fracture centers are typically placed within the domain using a stochastic process such as a Poisson or Markov process (Dershowitz and Einstein, 1988). A commonly used model is called the Baecher (1977) model (Long and Witherspoon, 1985; Warburton, 1980a; Warburton, 1980b). The Baecher model assumes circular or elliptical joint shapes. In the case of circular joints the size is determined by the joint radius Rj. Whereas the length of the maximum and minimum chords is used to determine the size of elliptical joints following the equation

$$C_a = \left\{ \left(1+\tan^2(\alpha)\right) / \left(1/C_{\max}^2 + \tan^2(\alpha)/C_{\min}^2\right) \right\}^{0.5} \tag{10}$$

for elliptical joints where C_a is a chord oriented at an angle from the maximum chord (Dershowitz and Einstein, 1988). Other models used less often in hydrogeologic investigations of fractures are the Venenziano (1978) model, the Dershowitz (1984) model, and the Mosaic Block Tessellation (Ambarcumjan, 1974) model which are all reviewed in detail by Dershowitz and Einstein (1988). Regardless of the fracture network model used, the next step is to generate the fracture planes as discs, as in the Baecher model, or as polygons, as in other models (Long and Witherspoon, 1985). The lengths of the radii of the discs are distributed lognormally, exponentially, or by a power law distribution most often because these distributions of trace lengths are found most commonly in the field (Long and Witherspoon, 1985, Dershowitz et al., 2004). To orient the planes in space, directional data distributions, also called spherical distributions, are used. The most common are the bivariate Fisher, Bingham, Normal distributions as well as the Uniform distribution (Long and Witherspoon, 1985; Dershowitz et al., 2004). Mardia (1972) and Fisher et al. (1987) give detailed explanations of many different directional data statistical distributions.

After the fractures are generated within the domain, flow through each individual fracture is calculated. Long and Witherspoon (1985), Rouleau and Gale (1987), and Dershowitz et al. (2004) assume flow through the complete fracture using the parallel plate conceptualization based on the work by Snow (1965) where fractures are assumed to behave like two smooth parallel plates of glass and flow is uniform throughout the area of the fracture plane. This conceptualization invokes the cubic law where

$$Q/\Delta h = C(2b)^3 \tag{11}$$

for steady and isothermal flow where C is a constant which equals

$$C = \left(\frac{2\pi}{\ln\left(r_e/r_w\right)}\right)\left(\frac{\rho g}{12\mu}\right) \tag{12}$$

for radial flow (Witherspoon et al., 1980). Long and Witherspoon (1985) used a semianalytical method to compute the flow within each fracture which assumes intersections act as either sources or sinks. This method requires less computing effort than a completely numerical method, but Cacas et al. (1990) found this method required more computing effort than available to the authors. Therefore, they developed a DFN model based on the work of Gentier (1986) who found that flow through fractures occurred more as “flow tubes” or channels than as planar flow especially under load. Flow was modeled as occurring through bonds that linked the centers of adjacent fractures (Cacas et al., 1990). To calculate flow between fractures across intersections, most models use global mass balance equations, which are then employed to calculate the flow between fractures across intersections (Long et al., 1982). Permeability and flow are calculated in a similar way as with continuum approach models; however, because fracture surface areas are known through the fracture network model, flow is calculated through the modeled fractures rather than averaged over the REV as with the continuum approach. One commonly used equation is Oda’s (1984) permeability tensor:

k_{ij} = 1/12 ($F_{kk}D_{ij}$-F_{ij}) (13)

where $F_{ij} = \frac{\pi\rho}{4}\int_0^{\infty}\int_0^{\infty}\int_{\Omega} r^2 b^3 n_i n_j E(n,r,b) d\Omega dr db$ (14)

r= diameter of the fracture; b is fracture aperture; ni and nj are the components of the unit normal vectors projected on the orthogonal reference axes, i=1,2,3 and j=1,2,3; E (n,r,b)d Ω drdt is the probability of the unit normals of (n,r,b) cracks where the function is defined over the half solid angle $\Omega/2$, ρ is the volume density of fractures.

$F_{kk} = F_{11} + F_{22} + F_{33}$ (15)

where F_{11}, F_{22}, and F_{33} are the values of the main diagonal of the fracture orientation tensor (Oda, 1984).

Numerous DFN models have been proposed in 1D, 2D, and 3D forms, using different methods to decrease the complexity or the computation time. However, if the fracture network can not be fully characterized, the practical application of these models is limited (Berkowitz, 2002). Complete characterization of a fracture network requires effective aperture, orientation, location, and size descriptions (Long and Witherspoon, 1985). For calibration, DFN approach models require much more data than continuum models (Berkowitz, 2002).

Despite the data requirements for DFN modeling these models have been successfully used in the field. Caine and Tomusiak (2003) used this type of model successfully in the Turkey Creek watershed, Colorado by modeling the intensity of fracturing, the number of fractures per unit line length. Digggins et al. (2006) used a DFN model to estimate the bulk permeability of a fractured aquifer.

Upscaling

Rounded outcrops and heterogeneous spatial distributions of fracture sets raise concerns about field measurements of fracture orientation. As a means of verification, field mapping can be extended with the use of remote sensing. Lineament extraction using aerial photographs of the watershed could be used to compare with the orientations measured in the field.

The term "lineament" was defined by O'Leary (1976) as "a mappable, simple, or composite linear feature of a surface, whose parts are aligned in a rectilinear or slightly curvilinear relationship and which differs distinctly from the pattern of adjacent features and presumably reflects a subsurface phenomenon". Lineaments can be more easily extracted from aerial photographs using directional and non-directional filters which enhance the visibility of linear features in an image. A convolution process is used to do this wherein a 3x3 matrix is selected at a point on the image where the process will begin. Each pixel in a digital image contains a digital number (DN). A DN is brightness value. Pixels are identified by row and column (Jensen, 2005). Beginning in the upper right the convolution matrix is placed over the pixels in the input image and the DN values in these pixels are multiplied by the values in the convolution matrix. The resulting 9 values are summed and then added to the central value in the original image.

This new value replaces the original DN value in the pixel. This process continues from left to right across the image, then down one row and back to the left side of the image where the process begins again for the next row until the entire image has been processed. Different convolution matrices accentuate lines is different directions. Expanding the 3x3 matrix to 5x5 or 7x7 can overcome any tendencies for bias to a particular direction resulting from the convolution matrix itself (Sabins, 2001).

The continuum approach model allows for both stochastic as well as deterministic calculation using simple averaging of the permeability. Heterogeneity, breaks in scale, and the existence of a REV are more easily seen when the model is used stochastically. Therefore, a Monte Carlo simulation of combined permeability with incrementally increased outcrop area enabled the observation of small scale heterogeneities as permeability was upscaled to the scale of the watershed. These heterogeneities and patterns could not be observed by simply combining the permeabilities of all the outcrops into a deterministic solution to the model for the watershed.

METHODS

Outcrop scale estimation of permeability

Field measurements were taken at 190 outcrops throughout the DCEW as well as several locations in the 8th Street Trenches (see Figure 1). These trenches were excavated perpendicular to slopes in the foothills north and northeast of the city of Boise to prevent mass wasting after a range fire in the area. The trenches were dug through the overburden to bedrock. In many locations excavation went through some bedrock, exposing fresh rock that had been exposed for less than one decade. Such locations allow for the measurement of fracture apertures which had been subjected to little weathering.

In contrast, outcrops in the DCEW are well rounded due to weathering and fracture apertures range from several millimeters to over a meter. So that permeability calculations could be performed for outcrops in the DCEW, apertures measured in the 8th Street Trenches were applied to fractures measured in the DCEW based on the orientation of the fracture plane. The determinant of the orientation tensor was calculated for fractures measured in the 8th Street trenches and for fractures in the DCEW and the aperture corresponding to a particular determinant was applied to the fractures in the DCEW. Linear interpolation was used to find the aperture in cases where the determinant of a fracture in the DCEW falls between determinants of fractures in the 8th Street trenches.

In the field, waypoints were taken using a Garmin eTrex Vista handheld global positioning unit to trace the circumference of each outcrop. A polygon shapefile was then created of the outcrop footprints in ArcGIS. Fractures were then drawn on hard copies of the outcrop maps, the maps were scanned and the fractures were digitized to a polyline shapefile. Digitizing outcrops and fractures enabled multiple realizations of permeability calculations. Sampling lines were drawn in each outcrop polygon in ArcGIS using a random number generator to create a line orientation between 1 and 360 degrees. The fractures intersecting each of the 190 sampling lines were extracted and used to calculate permeability along that line.

Fracture orientations were declared in the quadrant system to facilitate the conversion of strike directions to azimuths of normals to the planes. A convention of negative for planes striking to the northwest and positive for planes striking to the northeast was applied. Finally the azimuths of the normals were calculated by

$$SN = \begin{cases} if\ S > 0, 90 - S \\ if\ S < 0, -(90 - |S|) \end{cases} \tag{16}$$

$$DN = 90 - |D| \tag{17}$$

where S = strike of the plane, D = dip angle of the plane, SN = azimuth of the strike normal, DN = the dip of the normal to the plane (Bianchi and Snow, 1969). The direction cosines of the planes were then calculated by l = cos SN * cos DN (18)

m = sin SN * cos DN (19)

n = sin DN (20)

The direction cosines of the sampling line are calculated using the same conventions as those described above for the fractures and are calculated by

D1 = cos SLT * cos SLP (21)

D2 = sin SLT * cos SLP (22)

D3 = cos SLP (23)

where SLT and SLP are the sampling trend and plunge respectively (Bianchi and Snow, 1969).

Shapefiles of fractures and outcrops automated the process of choosing a sampling line and selecting the fractures which intersect the sampling line which would then be used to calculate the permeability and hydraulic conductivity of the fracture network along that line using the method described by Bianchi and Snow (1969). A line of any dimension aligned at any desired orientation could be created allowing for the detailed study of the effects of scale and the REV on the heterogeneity of hydraulic properties in a fractured medium.

Snow (1969) determined the equation for the equivalent permeability for each fracture:

$$k_{ij} = \frac{2}{3L}\frac{b^3}{\left|n_i D_i\right|}\left(\delta_{ij} - m_{ij}\right) \qquad (24)$$

where L is the length of the sampling line, b is the aperture, n_i and D_i are the direction cosines of the fracture plane and the direction cosines of the sampling line, δ_{ij} is the Kronecker delta, and m_{ij} is the orientation matrix of the normal to the conduit.

The equivalent permeability at an outcrop is the sum of the contribution of each fracture and the average of the values of all the outcrops in a region will give the equivalent permeability of the rock in that region.

$$\overline{K}_{ij} = \frac{1}{N}\sum\frac{2}{3L}\sum\frac{b^3}{|n_i D_i|}\left(\delta_{ij} - m_{ij}\right) \qquad (25)$$

Equation 24 is expanded to

$$\begin{bmatrix} k_{11} & k_{12} & k_{13} \\ k_{12} & k_{22} & k_{23} \\ k_{13} & k_{23} & k_{33} \end{bmatrix} = \frac{2b^3}{3L\begin{bmatrix} l \\ m \\ n \end{bmatrix} \bullet \begin{bmatrix} D_1 \\ D_2 \\ D_3 \end{bmatrix}} \begin{bmatrix} 1-ll & -lm & -\ln \\ -lm & 1-mm & -mn \\ -\ln & -mn & 1-nn \end{bmatrix} \qquad (26)$$

(Bianchi and Snow, 1969). This equation is used to calculate the contribution of each fracture to the permeability and the sum of the contributions of every fracture intersecting the sampling gives the permeability along that outcrop.

The eigenvalues of the permeability tensors at each outcrop give the principal permeabilities and the eigenvectors give the directions cosines of these principal permeabilities (Bianchi and Snow, 1969). The largest eigenvalue is the moment of inertia of the vectors around the first eigenvector and the sum of the squared distances from the tips of the vectors to the first eigenvector is the minimum. These values were used to perform Monte Carlo simulations of the permeability as it is an estimate of the mean permeability of that outcrop (Woodcock, 1977).

Upscaling Methods

To investigate the effects of heterogeneous spatial distributions of fracture sets and of measuring fracture orientation in rounded apertures field data was extended using lineament extraction of aerial photographs. This also would allow for the completion of the network characterization by providing length data for fractures.

For lineament extraction this investigation used 1:24,000 scale color infrared aerial photographs taken in the year 2000 for the PLSS coordinates 04N02E. The region analyzed within this mosaic was encapsulated by the UTM coordinates of 566339 by 573970 easting and 4844456 by 4837021 northing. These images were published by the Idaho Department of Water Resources. The spatial resolution of the photographs is 1.5 meters.

Twelve directional and one nondirectional filters were used to enhance linear features in the images: 3x3, 5x5, 7x7 horizontal edge detect; 3x3, 5x5, 7x7 vertical edge detect; 3x3, 5x5, 7x7 right diagonal edge detect; 3x3, 5x5, 7x7 left diagonal edge detect and 3x3 nondirectional edge detect. These filters were part of the Lieca Imagine software package for remotely sensed image processing. The images were imported to ArcMap 9.0 where lineaments were drawn on the output images to create a lineament shapefile.

The directions of these lines were measured in degrees from north to compare the orientations with those of field data.

To upscale permeability estimations a Monte Carlo simulation was used. The Monte Carlo simulation was done by first randomly selecting outcrops in groups. A random number generator in Microsoft Exel was used to select outcrops from the population in groups of 2, 5, 10, 15, 20, 25, and 50. Each selection was done ten times so that there were ten groups of 2 outcrops, ten groups of 5 outcrops, ten groups of 10 outcrops and so on resulting in 70 groups of increasing numbers of outcrops. The permeability for each simulation was calculated so that the permeability, for the first iteration, of two randomly selected outcrops were combined using Equation 25 ten times. The same was done using five outcrops randomly selected to create ten sets of five, and the same for ten outcrops and so on until 10 sets of outcrops had been selected using 2, 5, 10, 15, 20, 25, and 50 outcrops. The areas of these outcrops were then summed and plotted against the combined permeability.

RESULTS AND DISCUSSION

Field Reconnaissance

Figure 5 is a stereonet showing contours of poles to the fracture planes measured in the field. In 190 outcrops 966 fractures were measured for orientation. Weathering and censoring fractures prevented the measurement of fracture aperture and length in the field. This stereonet shows few fracture sets with very little clustering. This is the result of two possible effects: spatial heterogeneity of fracture sets in the watershed and/or the effect of weathered outcrops.

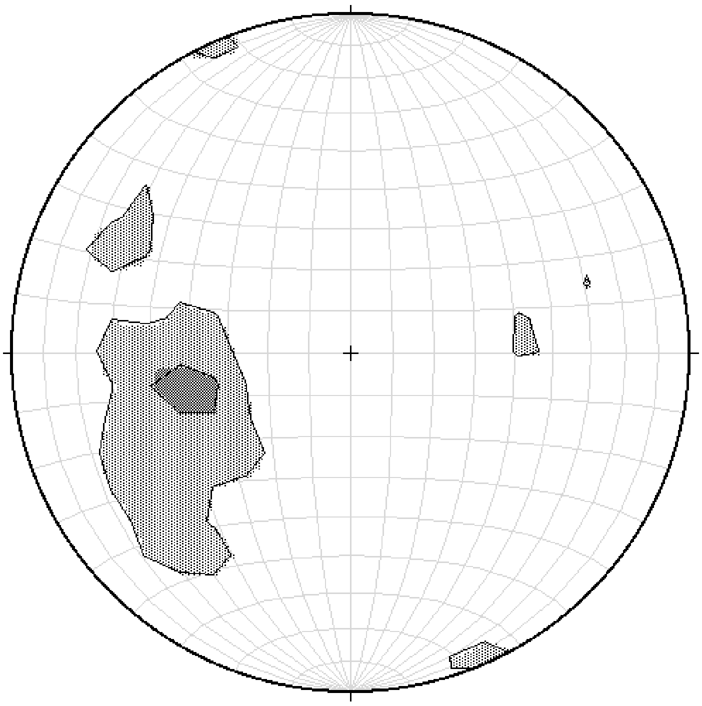

Figure 5: Stereonet of fracture orientations in the DCEW.

Figure 6 shows a map of sampling locations within the watershed and the stereonet of the fracture orientations at each region. Each region shows fracture sets that exhibit better clustering than when these sets are combined for the whole watershed. Typically fracture sets show increased clustering as additional fractures are measured while fractures in the DCEW showed the opposite phenomenon. This is likely a result of heterogeneous rock types throughout the watershed as areas of pegmatite and dikes have been identified in the watershed.

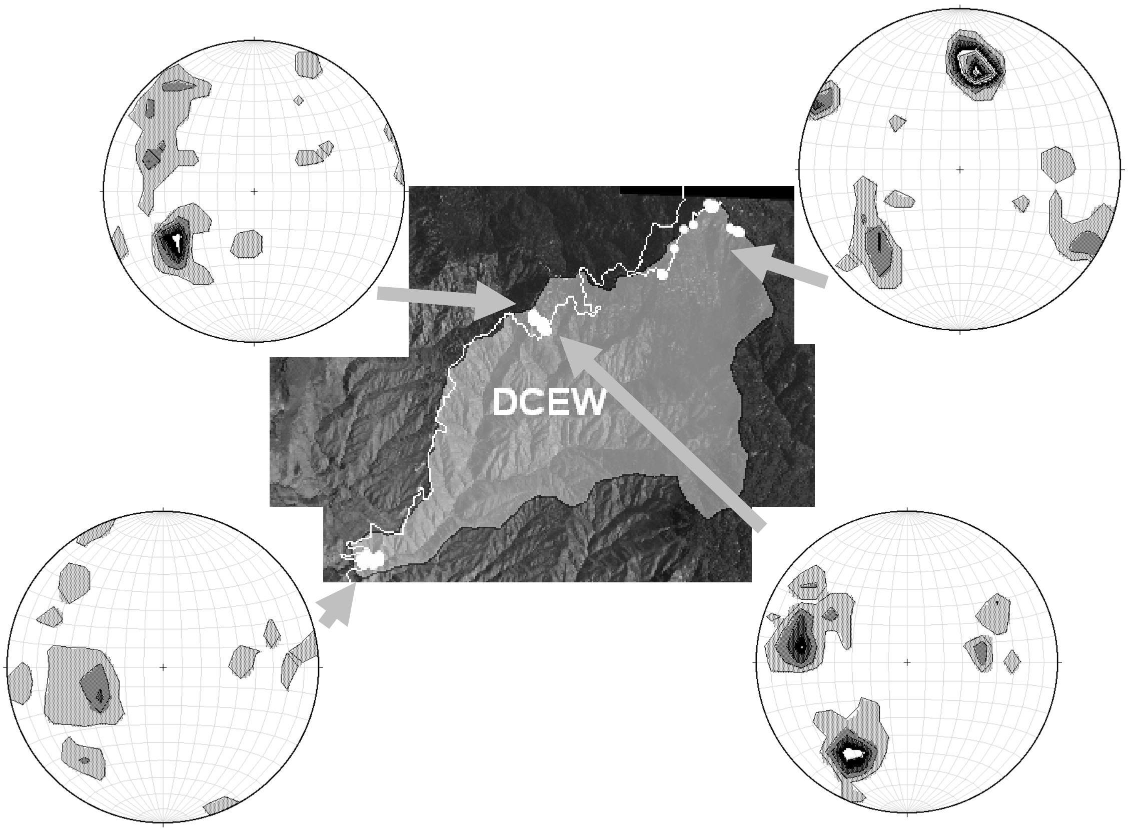

Figure 6: Spatial heterogeneity of fracture sets.

Weathering occurs to fracture apertures initially as these are exposed to fluid flow and represent weaker areas in the rock mass. Because of this, apertures are weathered more readily and become rounded. Orientation of fractures is measured in apertures and requires more care on rounded surfaces as does aperture measurement.

Figures 7 and 8 show the frequency distributions of the aperture for the 8th Street Trenches and the DCEW. Both data sets fit well to a power law distribution at apertures larger than about 7 mm. Apertures less than about 7 mm deviate from the power law distribution for both distributions. This is may be because as apertures become smaller, accuracy of measurement using a ruler decreases significantly. Another possible reason for this could be a threshold break resulting from grain size. The power law distribution is more typical for fracture apertures than the linear distribution.

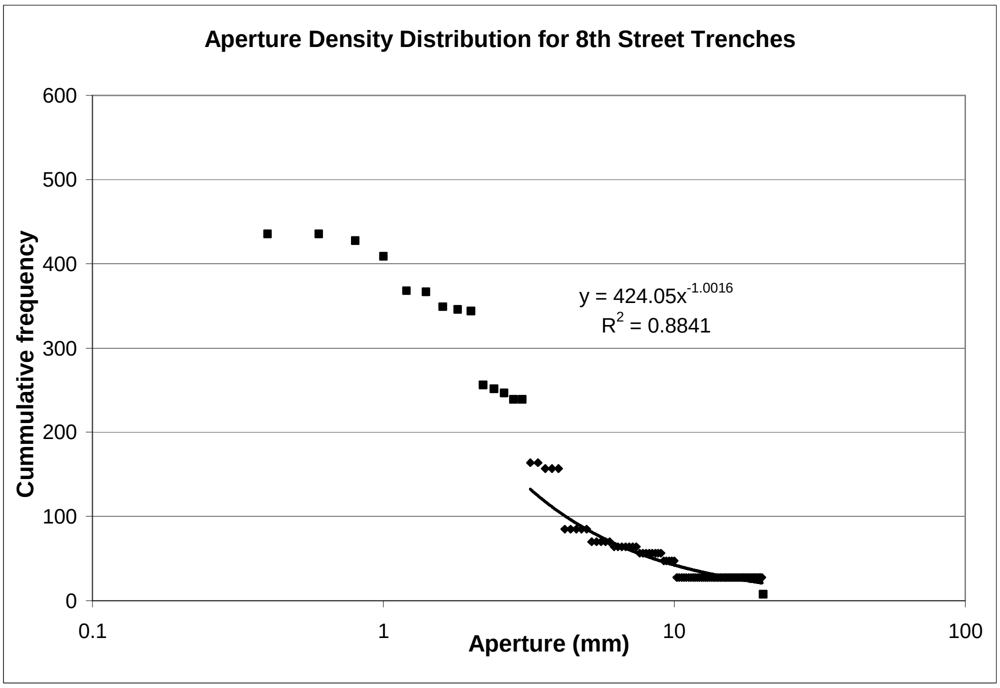

Figure 7: Density distribution of apertures measured in the 8th Street Trenches.

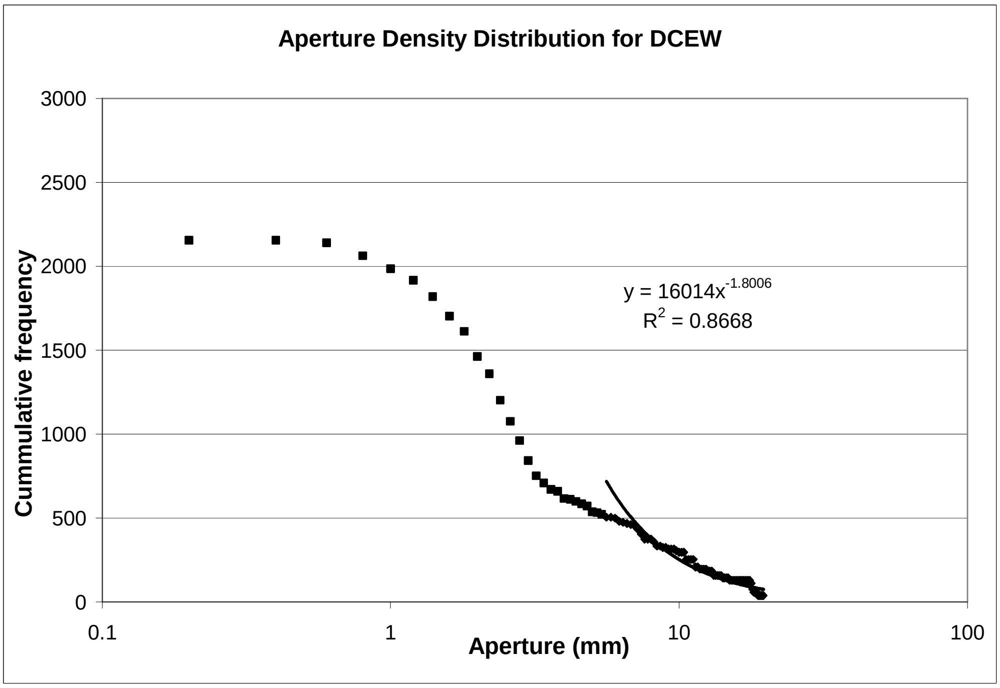

Figure 8: Density distribution of the apertures assigned to fractures in the DCEW.

Bianchi and Snow (1969) measured apertures in outcrops by photographing dyed fracture walls and enlarging the photographs. Using this technique they found and almost log-normal distribution while other authors (Barton and Zoback, 1992; Johnston and McCaffrey, 1996; Marrett, 1996) have found both log-normal and power law distributions with outcrop and core sample measurements. de Dreuzy et al. (2001b) surmised the discrepancy to be the result of homogenization within the fracture that transform power law distributions into log-normal distributions as log-normal distributions are generally calculated in hydraulic tests while geometric measurement most often results in a power law distribution. The linear distribution is anomalous and may be a result of a grain size strength threshold or a divergence from unweathered apertures to weathered apertures.

Table 1 compares aperture values measured in this investigation with those measured by other authors. It is clear from Equation 4 that fracture aperture plays an important role in governing the velocity of flow within a fracture; however, measuring aperture directly is difficult and inaccurate. Indirect measurement through hydraulic tests calculate aperture inversely using the cubic law. The aperture calculated using these types of methods is the “hydraulic aperture” which cannot be measured directly (McKay et al., 1993). Further complication in aperture measurement occurs because fracture walls are rough and covered with asperities of varying size and density, creating aperture widths that vary significantly over the length of the fracture. Also, fracture apertures are known through pump test data to decrease dramatically with depth (Snow, 1968). Renshaw (2000) surveyed the literature and found that reported apertures varied from several microns to several millimeters. Due to this complexity and because fracture apertures are difficult to accurately measure in the field, few investigations into aperture distributions exist compared to the voluminous information about fracture length distributions available (Bonnet et al., 2001).

Source	minimum aperture (m)	maximum aperture (m)
DCEW	4.00E-04	1.98E-02
Bianchi & Snow (1969)	1.22E-04	5.41E-04
Snow (1968)	1.25E-04	3.05E-04
Renshaw (2000)	2.00E-07	2.70E-03
Gundmundson et al. (2000)	0.00E+00	8.00E-03
McKay et al. (1993)	0.00E+00	4.50E-05

Table 1: Published ranges of apertures (in meters).

Outcrop Permeability Estimation

Table 2 shows a summary of the results of the continuum approach modeling done for outcrops in the DCEW, along with summary statistics of the outcrops areas. Figure 9 shows the permeability plotted against the outcrop area. This plot mimics the REV plot of Hubbert (1956) shown in Figure 2. A clear drawback to the data analysis presented in Figures 2 and 9 is that only a few large outcrops create the plateau.

outcrop area minimum (square meters)	outcrop area maximum (square meters)	outcrop area mean (square meters)	outcrop area standard deviation
0.35	752.13	42.75	105.16
permeability minimum (square meters)	permeability maximum (square meters)	permeability mean (square meters)	permeability standard deviation
8.94E-15	1.15E-06	2.14E-08	1.03E-07

Table 2: Tabulated results of stochastic permeability estimation.

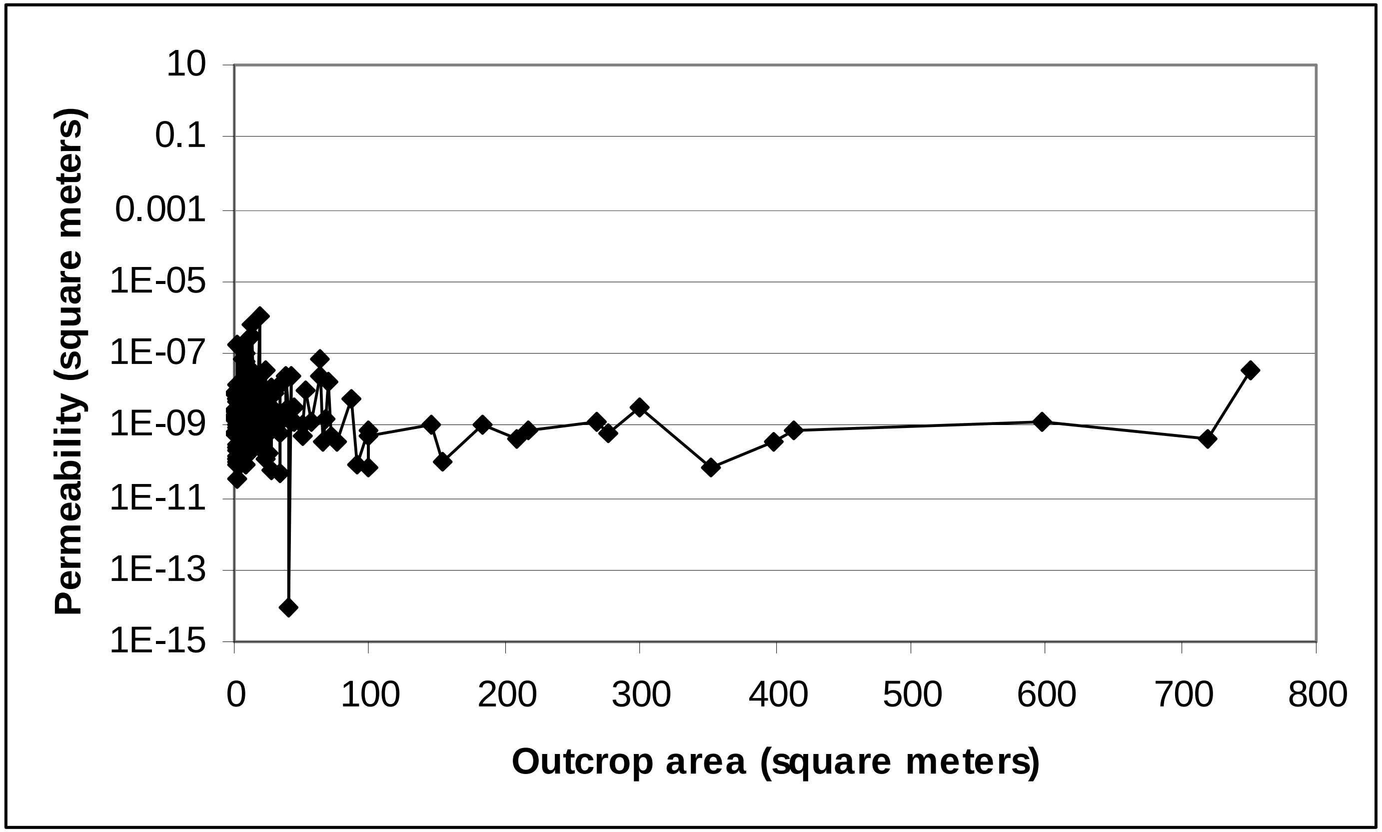

Figure 9: Permeability versus outcrop area plot mimicking Hubbert's (1956) plot.

The small outcrops display a great deal of heterogeneity that typifies hydraulic properties of fracture networks. The permeability of individual outcrops in DCEW ranges from 10^{-15} to 10^{-6} m^2, with a mean value of 2.14 x 10^{-8} m^2, and a standard deviation of 1.03 x 10^{-7}. To convert these values to hydraulic conductivity, the relationship $K=K_i(\rho g/\mu)$ is used (Fetter, 2001). This leads to a range of hydraulic conductivities from 10^{-8} m/s to 10^{1} m/s with a mean of 2.34 x 10^{-1} m/s, a mode of 3.52 x 10^{-1} m/s and a standard deviation of 1.13.

Few groundwater studies have been done in or around the DCEW and before this study the flow through the fracture network had only been modeled based on hydraulic tests. Gates et al. (1994) used aerial photographs to map lineaments so that wells could be installed. Pump tests modeled using the Jacob straight-line method calculated 6.82 x 10^{-5} m^2/s for the transmissivity of the aquifer. The Jacob straight-line method (also called the Cooper-Jacob or Jacob-Cooper straight line method) is a method for solving the Thiem equation for radial flow to a pumping well in a completely confined aquifer (Fetter, 2001).

Clayton and Megahan (1986) performed injection tests at 1.5 m intervals in 10 boreholes drilled in a north-south transect across much of the Atlanta Lobe of the Idaho Batholith which crosses near the DCEW. Saturated hydraulic conductivity values were calculated based on these tests. Cores were also tested in the laboratory using falling head permeameter tests. The saturated hydraulic conductivity values ranged from 0 to 1.98 x 10^{-5} m/s with a mean of 2.08 x 10^{-6} m/s and were calculated also using a solution to the Thiem equation for radial flow in a confined aquifer. To the author's knowledge, these are the only published hydrogeologic investigations performed in the bedrock of the Idaho Batholith.

With the two above investigations encompassing all published groundwater investigations, the typical shape of the hydraulic properties specific to the Atlanta Lobe of the Idaho Batholith are not well established. However, the permeabilities calculated for the DCEW fall slightly higher than the ranges established for fractured crystalline rocks. Illman (2006) compiled permeability measurements at various scales from published data and those published for granite and crystalline rocks ranged from 10^{-23} m^2 to 10^{-13} m^2. Hydraulic conductivity measurements reviewed by Gale (1982), Hseih (1998), and Renshaw (1999) are similar to hydraulic conductivities calculated here with a range of 10^{-12} m/s to 10^{-1} m/s.

Table 3 shows the mean and range of values of hydraulic conductivity reported for fracture networks in other investigations. The maximum hydraulic conductivity values calculated in this investigation are higher than those reported in other investigations however the minimum values are very similar to those found by Clayton and Megahan (1979) using hydraulic tests.

Source	measurement method	hydraulic conductivity minimum (m/s)	hydraulic conductivity maximum (m/s)
DCEW	mapping	9.77E-08	1.26E01
Clayton & Megahan (1979)	hydraulic and lab	1.97E-08	1.98E-05
Gates et al. (1994)	Hydraulic tests	0	1.24E-06
Hsieh (1998)	hydraulic tests	1.00E-12	1.00E-07
Snow (1968)	hydraulic tests	0	1.43E-11
Rouleau & Gale (1987)	mapping	2.80E-10	3.40E-04
McKay et al (1993)	multiple methods	1.00E-06	2.10E-04
Gale (1982)	multiple methods	4.91E-11	5.15E-06

Table 3: Published ranges of hydraulic conductivity (in m/s).

The high values may be a result of using the continuum approach; however, results from similar continuum models (Snow, 1969; Snow, 1968; Bianchi and Snow, 1969) are also lower than those calculated here. Gale (1982) compiled hydraulic conductivity values reported in literature using the continuum approach, and the range of these values falls below the upper limit and the mean of those for the DCEW. Aperture measurements used in the calculations by these authors are also considerably lower than those measured in the 8th Street Trenches and applied to fractures in the DCEW as illustrated in Table 1.

McKay et al (1993) noted that fracture apertures cannot be measured accurately in the field due to their small expected size and as a result of this most aperture measurements are inferred from hydraulic conductivity measurements using the cubic law. Similar difficulties were encountered during field reconnaissance for this investigation which may be partially responsible for the relatively large values. However, it is more likely that these fractures have been enhanced by significant weathering. These fractures were measured in areas where excavators were able to dig through the rock, indicating that weathering had weakened the crystalline rock making it rippable. This likely widened fracture apertures at least near the surface.

Upscaling

Lineament Extraction

Figure 10 shows the resulting map of the lineaments in DCEW. The frequency plot of the length of these features can be found in Figure 11. Removing the shorter fracture lengths, the distribution fits a power law as is most frequently found in fracture length investigations (Bonnet et al., 2001). The lengths range from 1.25m to 855.5m with a mean of 111.8m and a standard deviation of 66.7m.

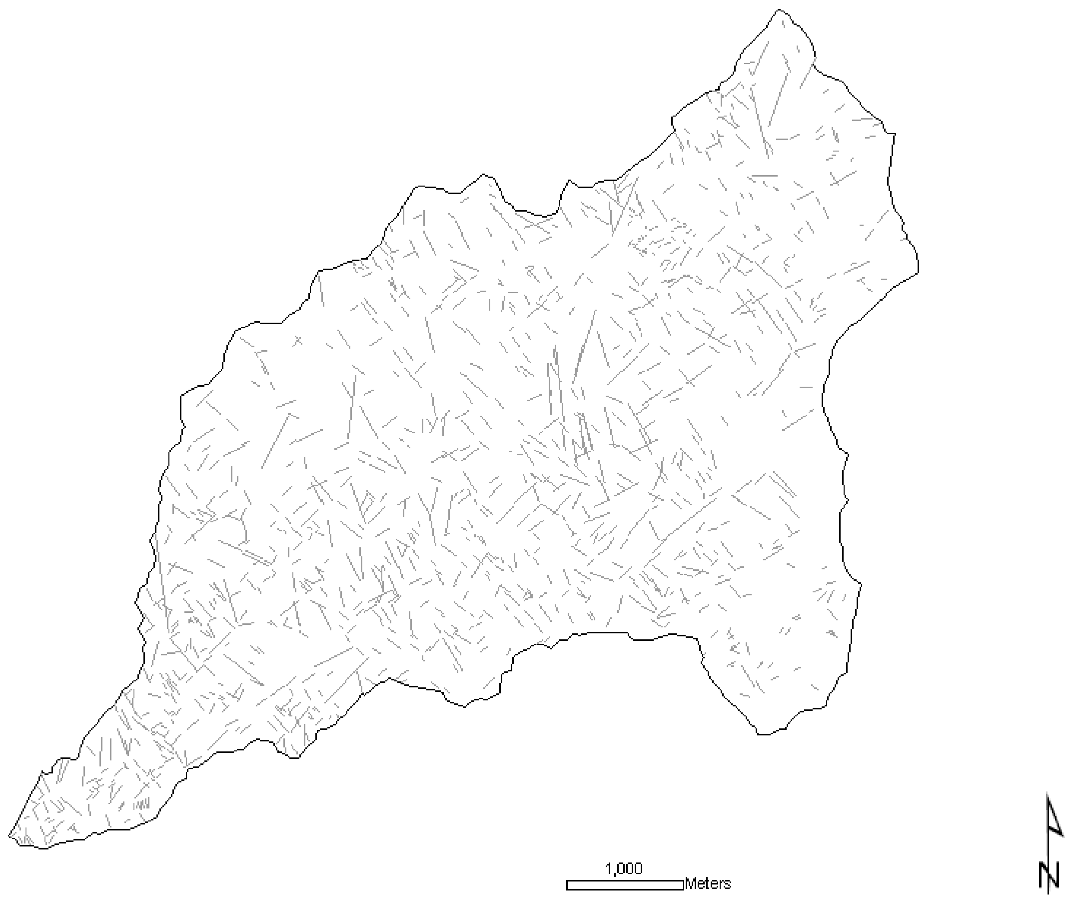

Figure 10: Lineament map.

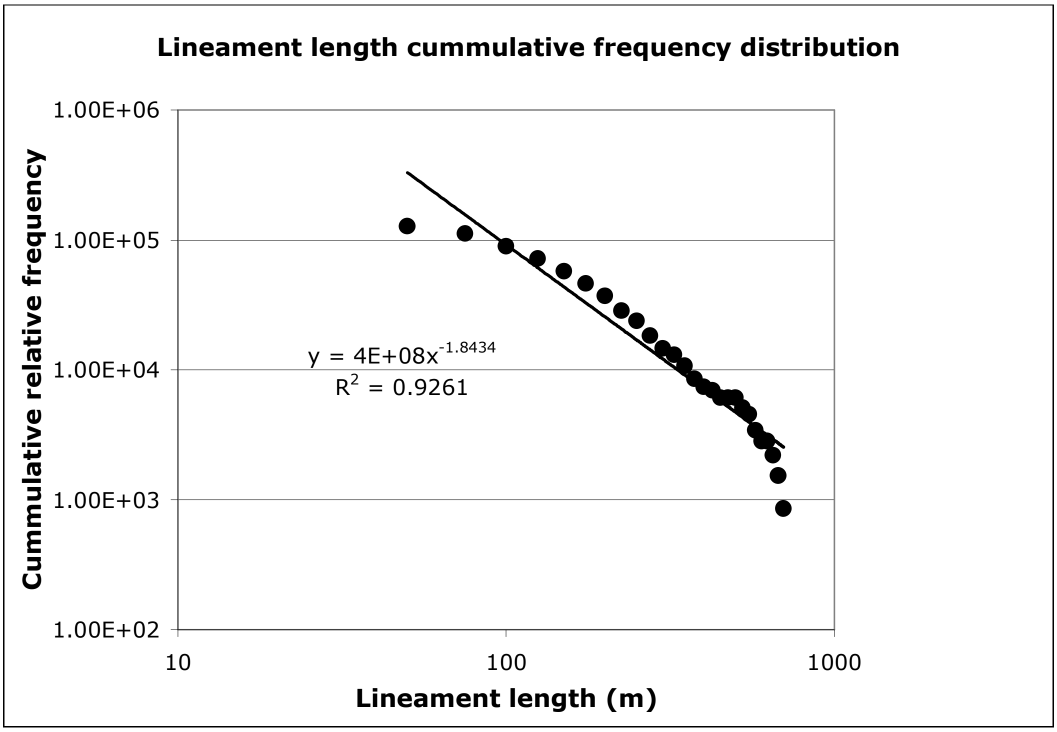

Figure 11: Lineament length cumulative relative frequency distribution.

The frequency of the lineament orientations are shown in Figure 12. The strike directions of the fractures are in the same plot for comparison. Because lineament data is only 2 dimensional, only the orientation of the line can be plotted. To simplify the plot, the directions are reported in the northern quadrants. For example a lineament or fracture plane striking 101 is included with those striking 281. The error bars on the lineament orientations are a result of the topographic correction on the lineaments.

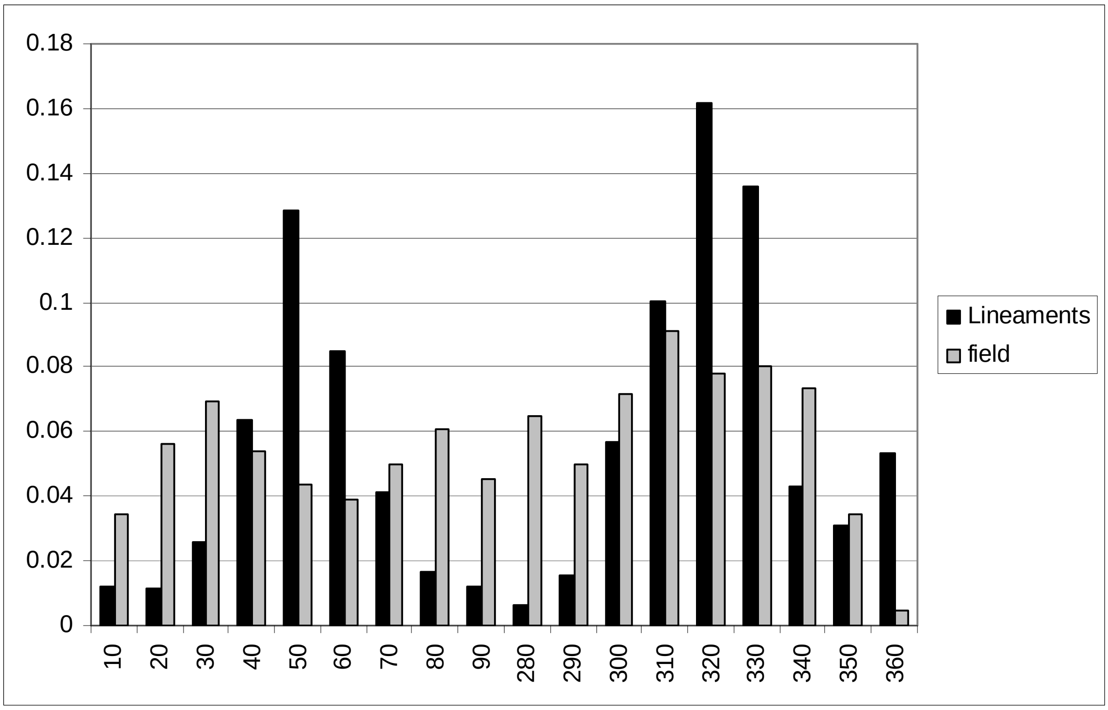

Figure 12: Lineament frequency distribution plot.

Lineaments show a similar distribution as the strike directions of fractures measured in the field. The approximately bimodal distribution has similar peaks indicating that field biases did not exclude any major fracture sets. Because orientations of lineaments and field mapped fractures are similar it may be true that no large break in scale exists and, therefore, combining outcrop permeabilities to increase the scale of observation such was done in the Monte Carlo simulations may be appropriate.

Lineaments are only a two dimensional trace resulting from a fracture plane intersecting topography as illustrated in Figure 13. As a result the strike directions of the fracture planes creating the lineaments could be far different than the orientation of the linear trace. While this is true, the agreement between the lineament orientations and fracture strike directions is remarkable. It is unlikely that the errors associated with the field measurements (heterogeneous fracture set spatial distribution and weathering) and the errors associated with the lineament orientation could combine to create two such similar bimodal distributions.

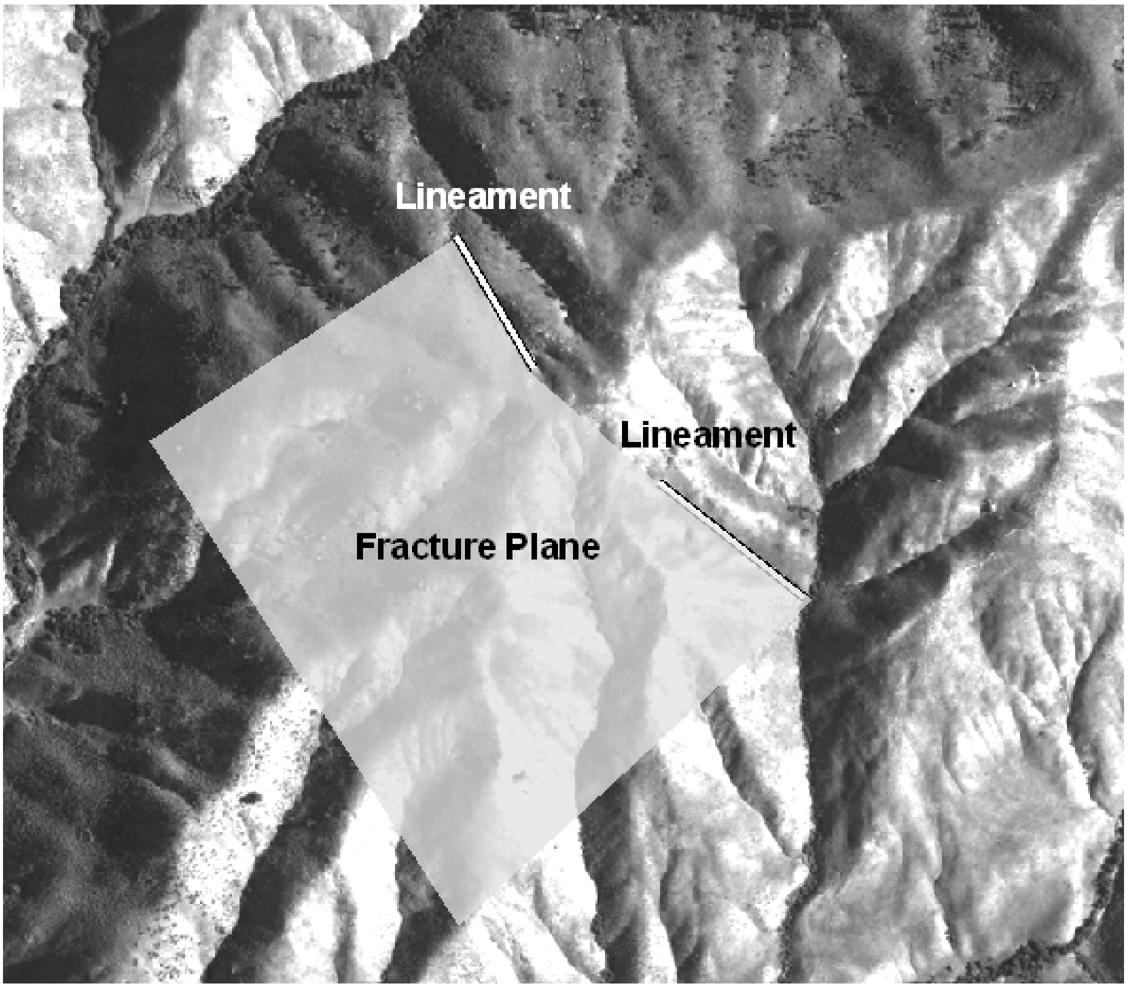

Figure 13: Illustration of topographic effect on lineaments.

A previous study by Gates et al. (1994) found 3 fracture sets in a region that surrounded and partially included the DCEW. These sets are oriented 20, 60NW; 290, 60SW; and 340, 60SW. The strike directions of these sets align closer to the high frequency strike directions of the field data better than the lineament directions.

Differences in orientations between field data and lineament data can result from a number of factors. The first influence is the change in scale. The same effect as seen in the concept of REV is often seen in fracture orientation patterns in that as scale increases fracture sets form much more distinct homogeneous sets. Thus as more and more fractures are measured distinct patterns mask local heterogeneities. Another aspect of this same concept is the simplification of a line that may have a serrated pattern in near-scale observation into a straight line in far-scale observation. Figure 14 illustrates this concept.

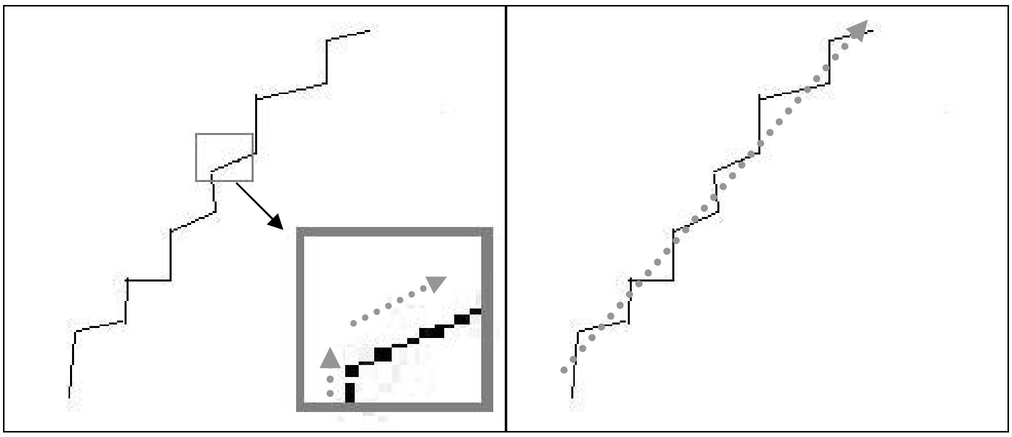

Figure 14: Effect of scale on fracture orientation. The first image shows a near-scale portion of the serrated line. The dashed gray arrows show possible orientation measurement directions. The second image shows the direction that would be measured in the far-scale view of the same line.

Monte Carlo Simulation

Figure 15 shows the results of Monte Carlo simulation of the permeability modeled using the continuum approach model. This figure shows a marked plateau at permeability $10^{-6}m^2$. The average of the values surrounding this plateau is $5.99 \times 10^{-7}m^2$ with a range of $1.19 \times 10^{-9}m^2$ to $1.57 \times 10^{-6}m^2$ for permeabilities of outcrops with area over 500 m^2. The permeability calculated deterministically is $1.49 \times 10^{-6}m^2$, just within the range determined stochastically. Table 3 compares these values with other investigations.

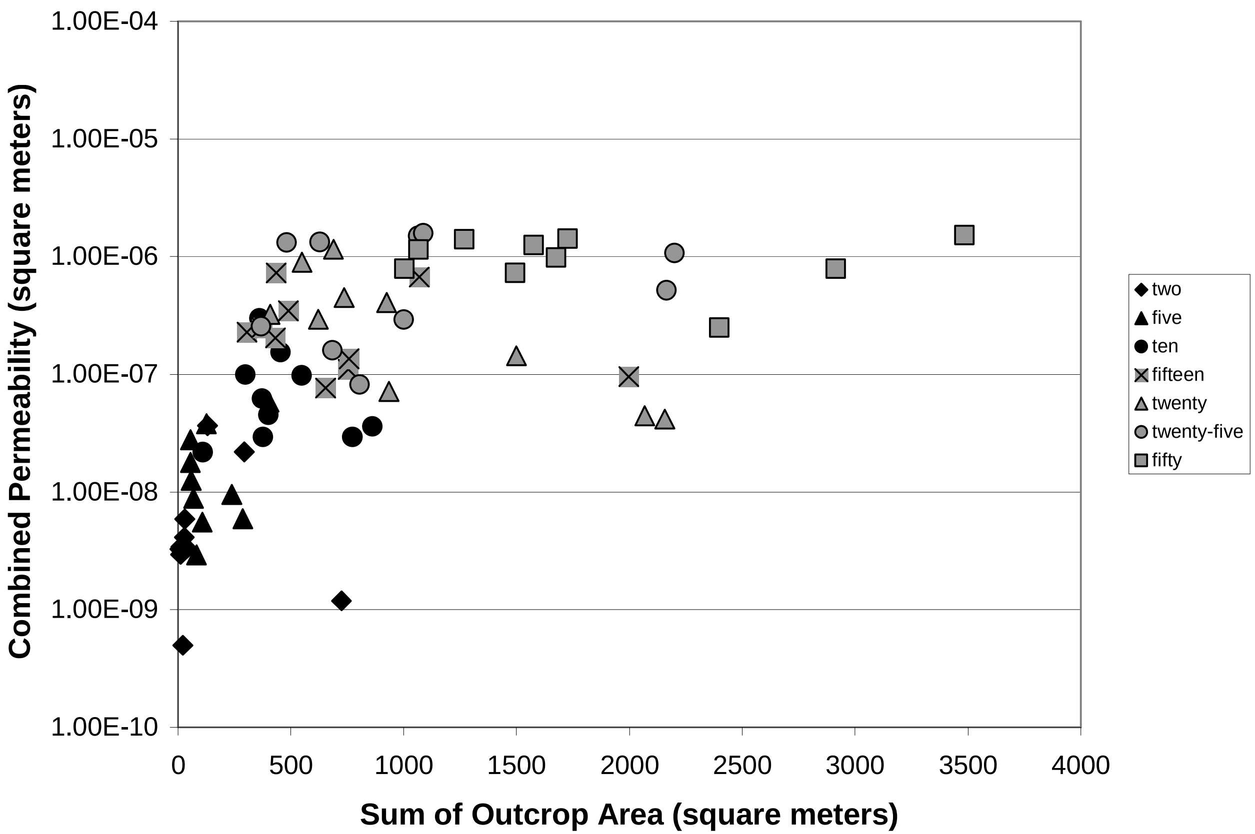

Figure 15: Monte Carlo simulation.

Another result of the data analysis is that a REV for the fracture network in the DCEW does exist. Therefore estimating an average permeability for the DCEW is possible. The plateau in Figure 15 occurs at about 1.00 x 10^{-6} m^2 which approximates a mean permeability for the watershed. Converting this to hydraulic conductivity results in 10.93 m/s. This mean permeability is larger than the mean of 1.00 x 10^{-9} m^2 (1.09 x 10^{-2} m/s as hydraulic conductivity) estimated using the traditional REV plot of Figure 9 and very similar to the mean of 1.49 x $10^{-6}$$m^2$ (hydraulic conductivity of 16.28 m/s) estimated deterministically using Equation 25.

Like Figures 2 and 9, a great deal of variability occurs in small outcrops, especially under about 700 m^2. A general rising trend exists as permeability increases with outcrop area however a maximum plateau is reached under 1000 m^2 of outcrop area. This plateau is made of many more measurements than for Figure 9.

The mean permeability values and, therefore, the hydraulic conductivity values determined using the Monte Carlo simulation are high for fractured, impermeable media. This is most likely because of the scale of measurement these values are determined over. When calculating the bulk permeability for an entire watershed the likelihood of encountering a large, highly conductive fracture is greater than for point scale measurements determined with hydraulic and laboratory investigations. Because the minimum hydraulic conductivity calculated here (9.77 x 10^{-8} m/s) agrees so well with point measurements determined using other techniques (1.97 x 10-8 m/s, Clayton and

Megahan (1979)), the use of continuum approach and the high apertures are not solely responsible for the enlarged permeability and hydraulic conductivity values.

CONCLUSIONS AND SUMMARY

Fracture aperture can vary over a broad scale and this is due to both chemical and physical erosion but also from normal pressure from the overburden (Bonnet et al., 2001). Previous investigations dealt with the difficulty in measuring aperture during field reconnaissance by applying a reasonable constant value (Caine and Tomusiak, 2003), by inferring aperture by fractal or scaling relationships between trace length and fracture aperture (de Dreuzy et al., 2002), or indirectly determined based on hydraulic conductivity (McKay et al., 1993). Because the data available at the DCEW was insufficient to completely characterize the fracture network, the aperture of the fractures was generated based on the orientations of fractures geographically near the DCEW, a region called the 8th Street Trenches. This technique has not been previously applied and future investigations will assess its viability.

To investigate possible field biases and to judge whether upscaling is appropriate for this fracture network, lineament extraction was performed. This was completed using arial photographs of the DCEW. Lineament orientations show a similar distribution to fracture strike directions measured in the field, therefore it is unlikely that field biases affected field data. Also, the similarity in the orientations of lineaments to those of fractures indicates that upscaling using the Monte Carlo simulation is appropriate.

The permeability and hydraulic conductivity of outcrops ranging in area from .35 m^2 to 752.13 m^2 was calculated using a continuum approach model. The results spanned several orders of magnitude for both permeability and hydraulic conductivity and the hydraulic conductivities were larger and more variable than previously reported values. The apertures of the fractures measured in the 8th Street Trenches were larger than those reported for many investigations and it is surmised that the crystalline bedrock containing these fractures had been subjected to considerable weathering as inferred from its rippability. The enlarged apertures have influenced the hydraulic modeling.

Monte Carlo simulations of permeability plotted with the outcrop area have several advantages over the classic REV diagram initially presented by Hubbert (1956). The Monte Carlo simulation results in many more measurements encompassing the larger scale portions of the plot. A plateau starting at about 500m^2 shows that an REV does exist for the DCEW. The permeability was determined stochastically from data presented by Figure 14 as well as deterministically with similar results. This result was much larger than the permeability determined using the classic Hubbert REV diagram. A clear decrease in variability of permeability with an increase in outcrop area is evident in the data while with using the Monte Carlo simulation this is not a result of fewer measurements available for larger outcrops. Continuum or effective porous media models can overestimate hydraulic properties derived with their use because the model assumes trace lengths that are the size of the REV. The atypically large hydraulic properties calculated for the DCEW may be a result of this effect however the similarly large aperture values seem to indicate that weathering of fracture apertures may have had a more pronounced affect. If this is true then permeabilities and hydraulic conductivities may be more applicable to infiltration studies than to deeper groundwater flow investigations. Future modeling using a DFN model will illuminate the real cause of the enlarged permeability values calculated in this investigation.

REFERENCES

Abdelmasih, D.M.M., 2006, Influence of saturated wedge hydrodynamics on hillslope-stream connectivity, Masters Thesis, Boise State University, Boise, Idaho, United States.

Aishlin, P., 2006, Groundwater recharge estimation using chloride mass balance, Dry Creek Experimental Watershed, Masters Thesis, Boise State University, Boise, Idaho, United States.

Ambarcumjan, R.V., 1974, Convex polygons and random tessellations *in* Harding, E.F. and Kendall, D.G. eds., Stochastic Geometry: John Wiley & Sons, New York, p. 176-191.

Baecher, G.B., Lanney, N.A., and Einstein, H.H, 1977, Statistical description of rock properties and sampling: Proceedings of the18th US Symposium on Rock Mechanics, p. SCI –I-SCI-B.

Barton, C.A., and Zoback, M.D., 1992, Self-similar distribution and properties of macroscopic fractures at depth in crystalline rock in the Cajon Pass Scientific Drill Hole: Journal of Geophysical Research, v. 97, n. B4, p. 5181-5200.

Bear, J., Tsang, C-F., de Marsily, G., 1993, Flow and Contaminant Transport in Fractured Rock: San Diego, California, Academic Press, 560p.

Berkowitz, B., 2002, Characterizing flow and transport in fractured geological media: a review: Advances in Water Resources, v. 25, p. 861-884.

Bianchi, L., and Snow, D.T., 1969, Permeability of crystalline rock interpreted from measured orientations and apertures of fractures: Annals of Arid Zone, v. 8, n. 2, p. 231-245.

Bonnet, E., Bour, O., Odling, N.E., Davy, P., Main, I., Cowie, P., and Berkowitz, B., 2001, Scaling of fracture systems in geological media: Reviews in Geophysics, v. 39, n. 3, p.347-383.

Cacas, M.C., Ledoux, E., de Marsily, G., Barbreau, A., Calmels, P., Gaillard, B., and Margritta, R., 1990, Modelling fracture flow with a stochastic discrete fracture network: calibration and validation, 2, the transport model: Water Resources Research, v. 26, no. 3, p. 491-500.

Caine, J.S. and Tomusiak, S.R.A., 2003, Brittle structures and their role in controlling porosity and permeability in a complex Precambrian crystalline-rock aquifer system in the Colorado Rocky Mountain Front Range: Geological Society of America Bulletin, v. 115, n. 11, p.1410-1424.

Clayton, J.L, Megahan, W.F., and Hampton, D., 1979, Soil and bedrock properties: weathering and alteration products and processes in the Idaho Batholith: USDA Forest Service Research Paper INT-237, 35p.

Clayton, J.L. and Megahan, W.F., 1986, Erosional and chemical denudation rates in the southwestern Idaho Batholith: Earth Surface Processes and Landforms, v.11, p. 389-400.

Criss, R.E., and Champion, D.E., 1984, Magnetic properties of granitic rocks form the southern half of the Idaho Batholith: influences of hydrothermal alteration and implications for aeromagnetic interpretation: Journal of Geophysical Research, v. 89, p. 7061-7076.

de Dreuzy, J.R., Davy, P., and Bour, O., 2002, Hydraulic properties of two-dimensional random fracture networks following power law distributions of length and aperture: Water Resources Research, v. 38, n. 12, p. 1-9.

Dershowitz, W.S., 1984, Rock Joint Systems, Ph. D. Thesis, Massachusetts Institute of Technology, Cambridge, Massachusetts.

Dershowitz, W.S., and Einstein, H.H, 1988, Characterizing rock joint geometry with joint system models: Rock Mechanics and Rock Engineering, v. 21, p. 21-51.

Dershowitz, W.S., Lee, G., Geier, J., Foxford, T., LaPointe, P.R., and Thomas, A., 2004, FracMan™, interactive discrete feature data analysis, geometric modling, and exploration simulation, version 4.0: Redmond, Washington, Golder Associates, User Documentation.

Digggins, J.P., Boutt, D., Manda, A.K., and Mabee, S.B., 2006, Estimating bulk permeability of fractured rock aquifers using detailed outcrop data and discrete fracture network modeling, Abstracts with Programs - Geological Society of America, v. 38, n. 7, pp.223.

Fetter, C.W., 2001, Applied Hydrogeology: Upper Saddle River, New Jersey, Prentice Hall, 598 p.

Fisher, N.I., Lewis, T., and Embleton, B.B.J., 1987, Statistical analysis of spherical data: Cambridge University Press, New York, pp. 329.

Gale, J.E., 1982, Assessing the permeability characteristics of fractured rock, in Narasimhan, T.N., ed., Recent trends in hydrogeology: Geological Society of America Special Paper 189, p. 163-181.

Gates, W.C.B., Parkinson, C.L., and Schroeder, K.L., 1994, Groundwater development in granitic terrain, Bogus Basin ski resort, Boise, Idaho in Link, P.K., ed., Hydrogeology, waste disposal, science and politics; proceedings of the 30th symposium on Engineering geology and geotechnical engineering, v. 30, p. 55-65.

Gentier, S., 1986, Morphologie et comportement hydromecanique d'une fracture naturelle dans un granite sous contrainte normale: Etude experimentale et theorique, these de doctorat, Universite d'Orleans, France.

Gudmundsson, A., 2000, Fracture dimensions, displacements and fluid transport: Journal of Structural Geology, v. 22, p. 1221-1231.

Hseih, P.A., 1998, Scale effects in fluid flow through fractured geologic media, *in* Sposito, G., ed., Scale dependence and scale invariance in hydrology: Cambridge, United Kingdom, Cambridge University Press, p. 335-353.

Hubbert, M.K., 1956, Darcy's law and the field equations of the flow of underground fluids, Transactions of the American Institute of Mining, Metallurgical, and Petroleum Engineers, v. 207, p. 222-239.

Hutchings, J., Petrich, C. R., 2002. Report: Groundwater recharge and flow in the regional Treasure Valley aquifer system: Geochemistry and Isotope Study. Submitted to The Idaho Department of Water Resources by The Idaho Water Resources Research Institute.

Illman, W.A., 2006, Strong field evidence of directional permeability scale effect in fractured rock: Journal of Hydrology, v. 319, p. 227-236.

Johnston, J.D. and McCaffrey, K.J.W., 1996, Fractal geometries of vein systems and the variation of scaling relationships with mechanism: Journal of Structural Geology, v.18, no.2/3, p. 349-358.

Long, J.C.S., Remer, J.S., Wilson, C.R., and Witherspoon, P.A., 1982, Porous media equivalents for networks of discontinuous fractures: Water Resources Research, v. 18, n. 3, p. 645-658.

Long, J.C.S., and Witherspoon, P.A., 1985, The relationship of the degree of interconnection to permeability in fracture networks: Water Resources Research, v. 90, n. B4, p. 3087-3098.

Manning, A.H., and Solomon, D.K., 2003, Using noble gases to investigate mountain-front recharge: Journal of Hydrology, v. 275, pp. 194-207.

Mardia, K.V., 1972, Statistics of directional data: Academic Press, New York, pp. 357.

Marrett, R., 1996, Aggregate properties of fracture populations: Journal of Structural Geology, v. 19, p. 169-178.

McKay, L.D., Cherry, J.A., and Gillham, R.W., 1993, Field experiments in a fractured clay till 1. hydraulic conductivity and fracture aperture: Water Resources Research, v.29, n. 4, p. 1149-1162.

O'Leary, D. W., Friedman, J. D., and Pohn, H. A, 1976, Lineament, linear, lineation: some proposed new standards for old terms: Geological Society of America Bulletin, v. 87, p. 1463-1469.

Renshaw,C.E., 1999, Connectivity of joint networks with power law length distributions: Water Resources Research, v. 35, n. 9, p. 2661-2670.

Renshaw, C.E., 2000, Fracture spatial density and the anisotropic connectivity of fracture networks in Faybishenko, B., Witherspoon, P.A., and Benso, S.M., eds., Dynamics of fluids in fractured rock: American Geophysical Union Geophysical Monograph 122, p. 203-211.

Rouleau, A., and Gale, J.E., 1987, Stochastic discrete fracture simulation of groundwater flow into an underground excavation in granite: International Journal of Rock Mechanics and Mining Sciences & Geomechanics Abstracts, v. 24, no. 2, p. 99-112.

Sabins, F., 1997, Remote sensing: principles and interpretation, 3rd edition: New York, W.H. Freeman and Company, 494 pp.

Snow, D.T., 1965, A parallel plate model of fractured permeable media, Ph.D. dissertation: University of California, Berkeley, 331 pp.

Snow, D.T., 1968, Rock fracture spacings, openings, and porosities: Proceedings of American Society of Civil Engineers, v. 94, p. 73-91.

Snow, D.T., 1969, Anisotropic permeability of fractured media: Water Resources Research, v. 5, n. 6, p. 1273-1289.

Sweetkind, D.S., and Blackwell, D.D., 1989, Fission-track evidence of the Cenozoic thermal history of the Idaho Batholith: Tectnophysics, v. 157, p. 241-250.

Venenziano, D., 1978, Probalistic model of joints in rock, unpublished manuscript, Massachusetts Institute of Technology, Cambridge, Massachusetts.

Warburton, P.M., 1980a, A stereological interpretation of joint trace data: International Journal of Rock Mechanics and Mining Sciences & Geomechanics Abstracts, v. 17, p. 181-190.

Warburton, P.M., 1980b, Stereological interpretation of joint trace data: influence of joint shape and implications for geological surveys: International Journal of Rock Mechanics and Mining Sciences & Geomechanics Abstracts, v. 17, p. 305-316.

Williams, C.J., 2005, Characterization of the spatial and temporal controls on soil moisture and streamflow generation in a semi-arid headwater catchment, Masters Thesis, Boise State University, Boise, Idaho, United States.

Witherspoon, P.A., Wang, J.S.Y., Iwai, K., and Gale, J.E, 1980, Validity of Cubic Law for fluid flow in a deformable rock fracture: Water Resources Research, v. 16, no. 6, p. 1016-1024.

Woodcock, N.H., 1977, Specification of fabric shapes using an eigenvalue method: Geological Society of America Bulletin, v. 88, n. 9, p. 1231-1236.

Yenko, M., 2003, Hydrometric and geochemical evidence of streamflow sources in the Upper Dry Creek Experimental Watershed, southwestern Idaho, Masters Thesis, Boise State University, Boise, Idaho, United States.

Zimmerman, R.W., and Yeo, I.W., 2000, Fluid flow in rock fractures: from the Navier-Stokes equations to the Cubic Law in Faybishenko, B., Witherspoon, P.A., and Benso, S.M., eds., Dynamics of fluids in fractured rock: American Geophysical Union Geophysical Monograph 122, p. 213-224.